Proceedings of the 5th WSEAS Int. Conf. on Software Engineering, Parallel and Distributed Systems, Madrid, Spain, February 15-17, 2006 (pp196-201)

Direct Torque Control of Double-Star Induction Motors

R. Zaimeddine[1], E.M. Berkouk[3]
[1]Department of Electrical Engineering
University of M'hammed Bougara, Boumerdes
ALGERIA
[3] laboratoire commande des processus
Ecole National Polytechnique, El Harache, Alger

Abstract - The object of this paper is to study a new control structure for sensorless double-star induction motors (DSIM) dedicated to electrical drives using a two-level voltage source inverter (VSI). The output voltages of PWM inverter can be represented by 8 space vectors in (d , q) plane, two zero vectors and six non-zero vectors which divide the (d , q) plane into 6 regions. Then the amplitude and the rotating velocity of the flux vector can be controlled freely, Both fast torque and optimal switching logic can be obtained. The selection is based on the value of the stator flux and the torque. A novel DTC scheme of double-star induction motors is proposed in order to develop a suitable dynamic. Compared to classical Field Oriented Control (FOC), which necessitates generally three feedback loops with PI regulators, a current-regulated PWM converter, and two coordinate transformations, Direct Torque Control (DTC) uses only a couple of hysteresis comparators to perform both torque and flux dynamic control [1]. The results obtained show superior performances over the FOC one without need to any mechanical sensor.

Key Words: Double-star induction motor, Direct torque control, Fast torque response, Sensorsless control, Voltage source inverter.

1 Introduction

The rapid development of the capacity and switching frequency of the power semiconductor devices and the continuous advance of the power electronics technology have made many changes in static power converter systems and industrial motor drive areas. The conventional GTO inverters have limitation of their dc-link voltage and switching frequency. Hence, double-star induction motors provide an attractive solution for high power process. The vector control of induction motor drive has made it possible to be used in applications requiring fast torque control such as traction [2]. In a perfect field oriented control, the decoupling characteristics of the flux and torque are affected highly by the parameter variation in the machine.

The scheme proposed in this paper is also based on direct torque and flux control of induction machines fed by two three-phase VSI using a switching table. In this method, the output voltage is selected and applied sequentially to the machine through a look–up table so that the flux is kept constant and the torque is controlled by the rotating speed of the stator flux. The direct torque control (DTC) is one of the actively researched control scheme which is based on the decoupled control of flux and torque providing a very quick and robust response with a simple control construction in ac drives[3],[4]. This type of system associated to the DSIM presents particular advantages to naval ship propulsion systems which rely on high power quality, survivable drives.

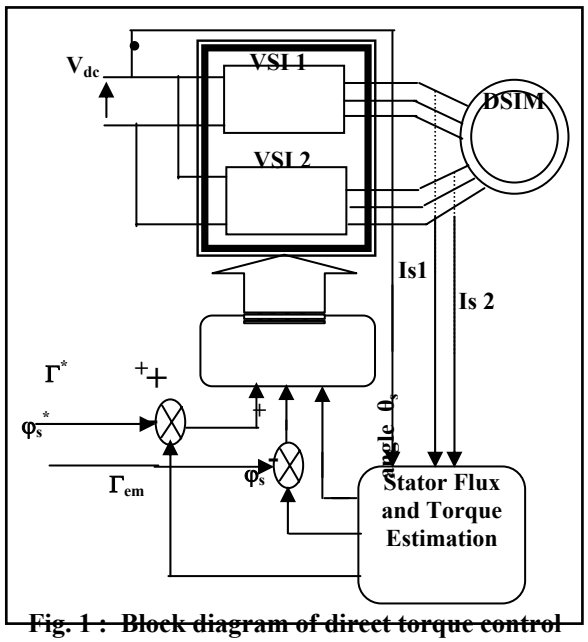

Fig. 1 : Block diagram of direct torque control

2 Converter DC/AC Model

Fig.2 shows the schematic diagram of two-level voltage source inverter (VSI), where Sa, Sb, Sc are switching function with value "1" when the switch is set to the positive voltage or "0" when the switch is set to the negative voltage. In this case, the voltage applied to the machine are determined only by the inverter switching mode and regarded as discrete values.

Table.1 shows the switching states of this inverter, since two kinds of switching states exist in each phase, a two-level inverter has 8 switching states.

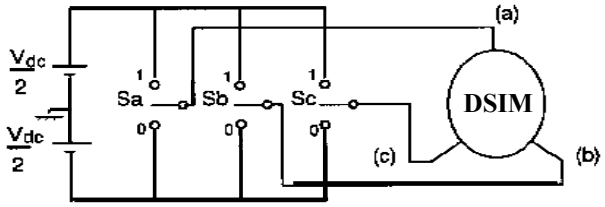

Fig. 2 : Schematic diagram of VSI Inverter

Switching states	S_a	S_b	S_c
V_0	0	0	0
V_1	1	0	0
V_2	1	1	0
V_3	0	1	0
V_4	0	1	1
V_5	0	0	1
V_6	1	0	1
V_7	1	1	1

Table 1: Switching states of VSI inverter

A two-level inverter is only capable to produce six non-zero voltage vectors and two zero vectors. Fig.5 shows the representation of the space voltage vectors for all switching states. The instantaneous vector of stator voltage can be expressed as follows:

$$\overline{V_s} = V_S . e^{j\theta_v} = \sqrt{\frac{2}{3}} . V_{dc} . e^{j.\frac{(k-1).\pi}{3}} \quad for\ k=1,2,....,6 \tag{1}$$

$$\overline{V_s} = 0 \qquad for\ k=0,7$$

$$\overline{Vs} = \sqrt{\frac{2}{3}}\, Vdc\ (Sa + a\,Sb + a^2\,Sc) \tag{2}$$

$$a = e^{j\frac{2\pi}{3}}$$

3 Modelling of a Double-Star Induction Motor

The double-star induction motor consists of a standard simple squirrel-cage rotor and two separate three-phase stator windings. The windings of the DSIM are shown in Fig.3.

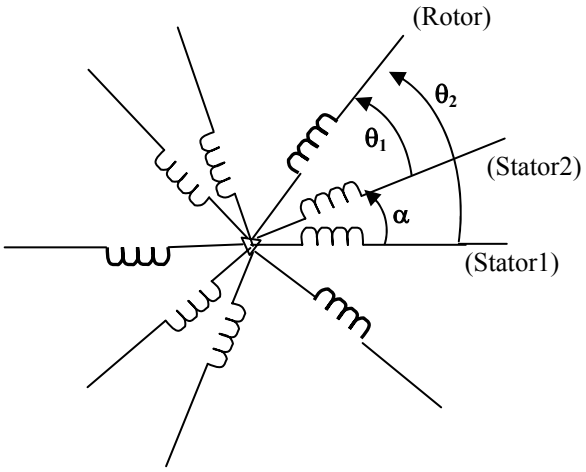

Fig.3 : Windings of the DSIM

The following assumptions are made :

- Motor windings are sinusoidally distributed,
- The two star have same parameters,
- Flux path is linear.

Since the two three phase windings wye-connected with isolated neutrals, zero-sequence harmonic currents are non-existent. So, only harmonics of order $3j \pm 1$ ($j=0,1,2,3\ldots$) are considered, by this way a complex model can be derived [5]. The scheme proposed in this paper is also based on direct torque control of DSIM, while being interested in the angle $\alpha=\pi/6$ or $\alpha=0$.

Torque control can be achieved on the basis of its model developed in a two axes (d , q) reference frame stationary with the stator winding, fig.4 . In this reference frame and with conventional notations (appendix), the electrical mode is described by the following equations:

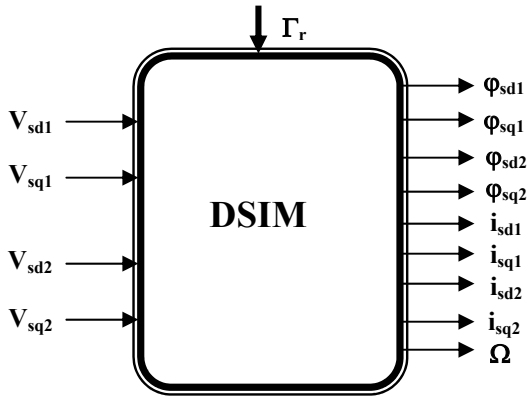

Fig. 4 : DSIM Model in the stationary reference

$$\frac{d\varphi_{sd1}}{dt}=V_{sd1}-R_{s1}i_{sd1} \quad (3)$$

$$\frac{d\varphi_{sq1}}{dt}=V_{sq1}-R_{s1}i_{sq1} \quad (4)$$

$$\frac{d\varphi_{sd2}}{dt}=V_{sd2}-R_{s2}i_{sd2} \quad (5)$$

$$\frac{d\varphi_{sq2}}{dt}=V_{sq2}-R_{s2}i_{sq2} \quad (6)$$

$$\varphi_{sd1}=L_{s1}\,i_{sd1}+L_m\left(i_{sd1}+i_{sd2}+i_{rd}\right) \quad (7)$$

$$\varphi_{sq1}=L_{s1}\,i_{sq1}+L_m\left(i_{sq1}+i_{sq2}+i_{rq}\right) \quad (8)$$

$$\varphi_{sd2}=L_{s2}\,i_{sd2}+L_m\left(i_{sd1}+i_{sd2}+i_{rd}\right) \quad (9)$$

$$\varphi_{sq2}=L_{s2}\,i_{sq2}+L_m\left(i_{sq1}+i_{sq2}+i_{rq}\right) \quad (10)$$

$$\varphi_{rd}=L_r\,i_{rd}+L_m\left(i_{sq1}+i_{sd2}+i_{rd}\right) \quad (11)$$

$$\varphi_{rq}=L_r\,i_{rq}+L_m\left(i_{sq1}+i_{sq2}+i_{rq}\right) \quad (12)$$

$$\Gamma_{em}=p\left[(i_{sq1}\varphi_{sd1}-i_{sd1}\varphi_{sq1})+(i_{sq2}\varphi_{sd2}-i_{sd2}\varphi_{sq2})\right] \quad (13)$$

The mechanical mode associated to the rotor motion is described by :

$$J\frac{d\Omega}{dt}=\Gamma_{em}-\Gamma_r(\Omega) \quad (14)$$

$\Gamma_r(\Omega)$ and Γ_{em} are respectively the load torque and the electromagnetic torque developed by the machine.

4 Stator Flux and Torque Estimation

Basically, DTC schemes require the estimation of the stator flux and torque. The stator flux evaluation can be carried out by different techniques depending on whether the rotor angular speed or (position) is measured or not. For sensorless application, the "voltage model" is usually employed [6]. The stator flux can be evaluated by integrating from the stator voltage equation.

$$\varphi_S(t)=\int(Vs-R_S I_S)dt \quad (15)$$

This method is very simple requiring the knowledge of the stator resistance only. The effect of an error in $R_s.i_s$ usually quite negligible at high excitation frequency but becomes more serious as the frequency approaches zero [6].

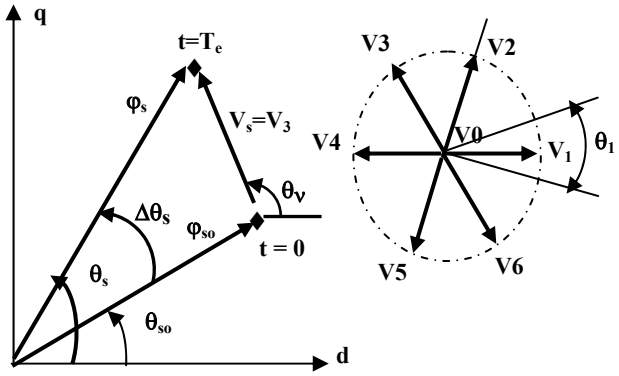

Fig. 5 : Flux deviation

The deviation obtained as the end of the switching period Te can be approached by the first order Taylor Seri as below.

$$\Delta\varphi_s \approx V_s.T_e.\cos(\theta_v-\theta_s)$$
$$\Delta\theta_s \approx T_e.\frac{V_s.\sin(\theta_v-\theta_s)}{\varphi_{so}} \quad (16)$$

Considering the combination of states of switching functions Sa, Sb, Sc. Fig.5 shows the adequate voltage vector selection we can increase or decrease the stator flux amplitude and phase to obtain the required performances. The electric torque is estimated from the flux and current information as [1]:

$$\Gamma_{em1}=p\,(i_{sq1}\varphi_{sd1}-i_{sd1}\varphi_{sq1}) \quad (17)$$

5 Principle Of Direct Torque Control

Fig.1 shows a block diagram of the DTC scheme. The reference values of flux, φs^* , and torque, $\Gamma_{em}{}^*$, are compared to their actual values and the resultant errors are fed into a two level comparator of flux and torque.

The stator flux angle, θ_s is calculated by :

$$\theta_S=\arctan\frac{\varphi_{sq}}{\varphi_{sd}} \quad (18)$$

And quantified into 6 levels depending on which sector the flux vector falls into. Different switching strategies can be employed to control the torque according to whether the flux has to be reduced or increased. Each strategy affect the drive behavior in terms of torque and current ripple, switching frequency and two or four-quadrant operation capability. Assuming the voltage drop $R_s.i_s$ small, the head of the stator flux φ_S moves in the direction

of stator voltage V_s at a speed proportional to the magnitude of V_s according to

$$\Delta\varphi_S = V_s\, T_e \qquad (19)$$

The switching configuration is made step by step, in order to maintain the stator flux and torque within limits of two hysteresis bands. Where T_e is the period in which the voltage vector is applied to stator winding. Selecting step by step the voltage vector appropriately, it is then possible to drive φ_s along a prefixed track curve.
Assuming the stator flux vector lying in the k-th sector (k=1,2,3,4,5,6) of the (d , q) plane, in the case of two level inverter, to improve the dynamic performance of DTC at low speed and to allow four-quadrant operation, it is necessary to involve the voltage vectors V_{K-1} and V_{K-2} in torque and flux control. In the following, V_{K-1} and V_{K-2} will be denoted "backward" voltage vectors in contraposition to "forward" voltage vectors utilised to denote V_{K+1} and V_{K+2}. A simple strategy which makes use of these voltage vectors is shown in table 2.

	$\Gamma_{em}\uparrow$	$\Gamma_{em}\downarrow$
$\varphi_s\uparrow$	V_{K+1}	V_{K-1}
$\varphi_s\downarrow$	V_{K+2}	V_{K-2}

Table 2: Selection strategy for four-quadrant operation

For steady operating conditions, equations (17) describing the machine torque can be transformed to a sinus function :

$$\Gamma_{elmo} = \Gamma_{max\,o}.\sin 2\gamma_o \qquad (20)$$

$\Gamma_{max\,o}$ *and* γ_o are equation respectively torque and the difference angle between stator and rotor flux vectors.

$$\Gamma_{max\,o} = p.\frac{1-\sigma}{2.\sigma.L_s}.\varphi_{so}^2 \quad ; \quad \gamma_o = \theta_{so} - \theta_{ro} \qquad (21)$$

Equations (20) and (21) are established with the assumption that stator flux and rotor closed values in steady state. For disturbed states, the stator flux angle θ_s has in practice a fast dynamic mode as compared to the rotor flux angle θ_r. If these two assumptions are hold the effect of stator vector voltage on the machine torque can be expressed by the first order Taylor expansion as below :

$$\Delta\Gamma_{elm} \approx K_\varphi.\Delta\varphi_s + K_\theta.\Delta\theta_s \qquad (22)$$

The sensitivity coefficients Kφ et Kθ are defined by :

$$\begin{cases} K_\varphi = \dfrac{d\Gamma_{elm}}{d\varphi_s} = \dfrac{2}{\varphi_{so}}.\Gamma_{elmo} \\ K_\theta = \dfrac{d\Gamma_{elm}}{d\theta_s} = 2.\Gamma_{max\,o}.\cos 2\gamma_o \end{cases} \qquad (23)$$

linking equations (16), (22) and (23) leads to :

$$\Delta\Gamma_{elm} = 2.\frac{V_s.T_e}{\varphi_{so}}.\Gamma_{elmo}.\cos(\theta_v - \theta_{so}) + \frac{2.V_s.T_e}{\varphi_{so}}.\sqrt{\Gamma_{max\,o}^2 - \Gamma_{elmo}^2}.\sin(\theta_v - \theta_{so}) \qquad (24)$$

This shows the feasibility torque control by a well selected vectors voltage $\overline{Vs}$ [7].
According to this strategy, the stator flux vector is required to rotate in both positive and negative directions. By this, even at very low shaft speed, large negative values of rotor angular frequency can be achieved, which are required when the torque is to be decreased very fast. Furthermore, the selection strategy represented in table.2 allows good flux control to be obtained even in the low speed range. However, the high dynamic performance which can be obtained utilising voltage vectors having large components tangential to the stator vector locus implies very high switching frequency.

6 Switching Strategy

The switching strategy in the order of the sector θs, is illustrate by table 3. The flux and torque control by vector voltage has in nature a desecrate behavior. In fact, we can easily verify that the same vector could be adequate for a set of value of θ_s. The number of sectors should be as large as possible to have an adequate decision.
The appropriate vector voltage is selected in the order to reduce the number of commutation and the level of steady-state ripple.

Sectors (θ_s)			1	2	3	4	5	6
ccpl	1	cflx	1	V2	V3	V4	V5	V6	V1
			0	V3	V4	V5	V6	V1	V2
ccpl	0	cflx	1	V6	V1	V2	V3	V4	V5
			0	V5	V6	V1	V2	V3	V4

Table 3 : Switching Strategy

For flux control, let the variable E_φ ($E_\varphi=\varphi_s^*-\varphi_s$) be located in one of the three regions fixed by the contraints:

$$E_\varphi < E_{\varphi\,min}\ ,\ E_{\varphi\,min} \le E_\varphi \le E_{\varphi\,max}\ ,\ E_\varphi > E_{\varphi\,max}\ .$$

The switable flux level is then bounded by $E_{\varphi\,min}$ and $E_{\varphi max}$. The regions defined for torque location are also noted by :

$$E_\Gamma < E_{\Gamma min}\ ,\ E_{\Gamma min} \le E_\Gamma \le E_{\Gamma max}\ ,\ E_\Gamma > E_{\Gamma max}$$

And then controlled by an hysteresis comparator. We apply the principle of the control while estimating the flux and the couple of every stators, what allows us to get an equivalent machine with the made previously assumptions.

7 The Simulation Results

The validity of the proposed DTC algorithm for three-phase voltage source inverter is proved by the simulation results using Matlab-Simulink. The parameters of motors are given in the Appendix. The used flux and torque mismathes for the approach are expressed in percent with respect to th flux and torque reference values.

$E_{\varphi\,max}$ = 2.14 % , $E_{\varphi\,min}$ = - 2.14 % , $E_{\Gamma min}$ = - 2.5 % , $E_{\Gamma max}$ = 2.5 %.

The simulation results illustrates both the steady state and the transient performance of the proposed torque control scheme. However, the machine has been supposed to run at load.

$$\Gamma r=\left(\frac{\Gamma em}{\Omega ref}-K_f\right).\Omega \qquad (25)$$

Fig.6 shows the phase current and flux for steady state operation and transient régime at 14 N.m with 1.4 Wb. The wave form of the stator current is closed to a sinusoidal signal. The trajectory of the flux in the case of α=0° is nearly a circle and answers more quickly compared to the flux response in the case of α=30°.

The phase current generated by the three-phase inverter have low harmonic components. Fig.8 shows the current harmonics in the phase Isa1 (11.50 % THD).

Low torque ripple is observed in the fig.6 and fig.7. One nearly has the same rate of harmonic for the two approaches.

Fig.9 shows the torque reverse response from + 14 N.m to - 14 N.m and flux for 1.4 Wb. The output torque reaches the new reference torque in about 1ms, fast torque response is obtained.

From this analysis high dynamic performance, good stability and precision are achieved.

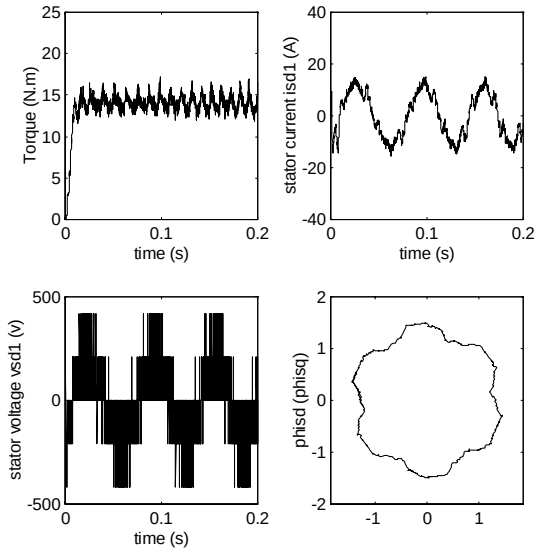

Fig. 6 Torque response, stator current in the phase Sa1 stator voltage, vector flux locus for α=30°

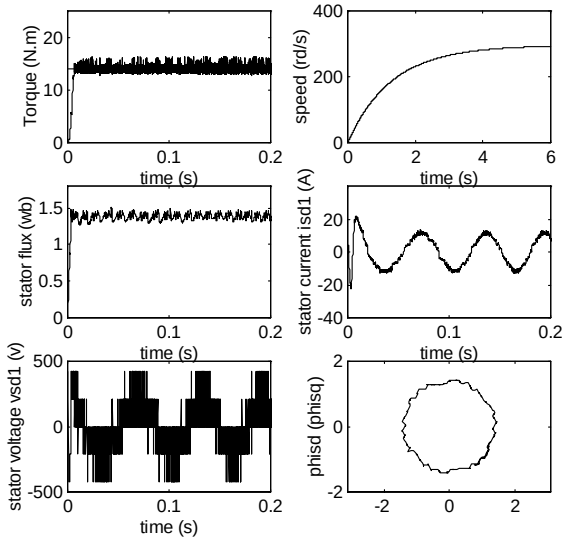

Fig. 7 Torque, flux, speed response, stator current in the phase isa1, Stator voltage, vector flux locus for α=0°

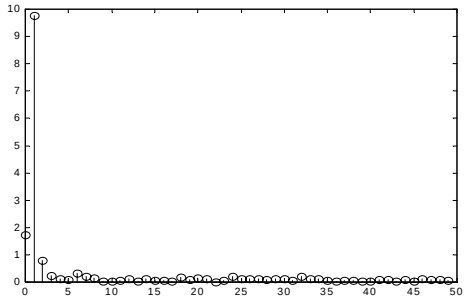

Fig. 8 : Current harmonics Isa1

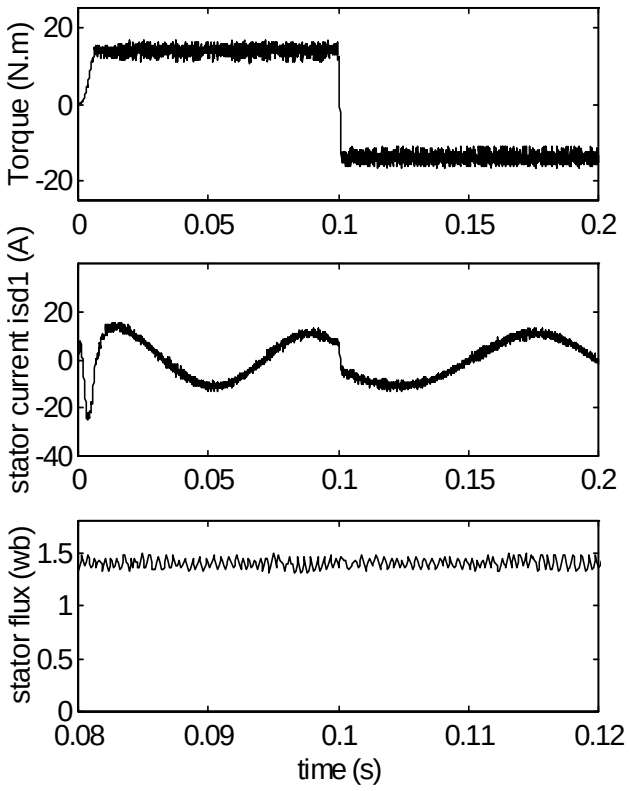

Fig. 9 Stator current in the phase sa1, flux response and electric torque reverse response of the motor for α=0°

8 Conclusions

The direct torque control DTC was introduced to give a fast and good dynamic torque and can be considered as an alternative to the field oriented control FOC technique.

High reliability is required, the in-line diagnosis or off-line diagnosis have to be considered in the case of the control using the field-oriented control. For this reason, The simulation results illustrates the feasibility torque control using a two three-phase inverter.

Two problems usually associated with DTC drives which are based on hysteresis comparators are: variable switching frequency and inaccurate stator flux estimation which can degrade the drive performance. The effect of proposed method has been proven by simulations. It is concluded that the proposed control produces better results for transient state operation then the conventional control.

In this paper, a DTC systems is presented it is suitable for high-power and high-voltage applications.

Appendix

Induction Motors Parameters

Rated power : 4.5 kW
Rated voltage : 220 V
Rated speed : 2840 rpm
Rated frequency : 50 Hz
Rotor resistance R_r : 2.12 Ω
Stator inductance L_{s1} : 0.011 H
Stator inductance L_{s2} : 0.011 H
Rated current : 6.5 A
Stator resistance $R_{s1} = R_{s2}$: 1.86 Ω
Rotor inductance : 0.274 H
Magnetizing Inductance : 0.3672 H
Number of pairs of poles : p = 1
Rotor inertia : 0.0625 Kg.m^2
Friction Coefficient : 0.008 N.m.s/rd
Sampling time Te : 100 μs
dc-link voltage V_d : 514 V

References

[1] I. Takahashi and T. Noguchi, "A new quick-response and high-efficiency control strategy of an induction motor". *IEEE Trans. on IA,* vol. 22, No. 5, Sept\Octo 1986, pp. 820-827.

[2] R. Zaimeddine, and E.M. Berkouk, "A Novel DTC scheme for a three-level voltage source inverter with GTO thyristors". *SPEEDAM 2004, Symposium on power electronics, electrical drives, automation & Motion, June,* vol. 2, June, 16th-18th 2004, pp. F1A-9-F1A-12.

[3] J.C. Trounce, S.D. Round, and R..M. Duke, "Comparison by simulation of three-level induction motor torque control schemes for electrical vehicle applications". *Proc. of international power engineering conference,* vol. 1, May 2001, pp. 294-299.

[4] WU. Xuezh, and L. Huang, "Direct torque control of three-level inverter using neural networks as switching vector selector". *IEEE IAS, annual meeting*, 30 September\ 04 October 2001.

[5] D. Hadiouche, H. Razik and A. Rezzoug, "Modeling of a double star-induction motor with an arbitrary shift angle between its three phase windings". Proc. EPE-PEMC'2000, Kosice, Solvak Republic, 5-7 September 2000.

[6] D. Casadei, G. Grandi, G. Serra, and A. Tani, "Switching strategies in direct torque control of induction machines". *ICEM 94*, vol. 2, 1994, pp. 204-209.

[7] F. Bacha, A. sbai, and R. Dhifaui, "Tow Approaches For Direct Torque Control of an Induction Motor". *CESA Symposium on control*, vol. 1, March 1998, pp. 562-568.